Tectonophysics 633 (2014) 115–125

Contents lists available at ScienceDirect

Tectonophysics

journal homepage: www.elsevier.com/locate/tecto

The 1998 Faial earthquake, Azores: Evidence for a transform fault associated with the Nubia–Eurasia plate boundary?

F.O. Marques [a,*], J. Catalão [b], A. Hildenbrand [c,d], A.C.G. Costa [b,c], N.A. Dias [b,e]

[a] Universidade de Lisboa, Lisboa, Portugal
[b] IDL, Universidade de Lisboa, Lisboa, Portugal
[c] Université Paris-Sud, Laboratoire IDES, UMR8148, Orsay F-91405, France
[d] CNRS, Orsay F-91405, France
[e] Instituto Superior de Engenharia de Lisboa, Lisboa, Portugal

ARTICLE INFO

Article history:
Received 19 March 2014
Received in revised form 4 June 2014
Accepted 22 June 2014
Available online 28 June 2014

Keywords:
Azores Triple Junction
1998 Faial earthquake
Transform fault
Block rotation and fault termination
Faial Graben
Terceira Rift

ABSTRACT

With very few exceptions, M > 4 tectonic earthquakes in the Azores show normal fault solution and occur away from the islands. Exceptionally, the 1998 shock was pure strike-slip and occurred within the northern edge of the Pico–Faial Ridge. Fault plane solutions show two possible planes of rupture striking ENE–WSW (dextral) and NNW–SSE (sinistral). The former has not been recognised in the Azores, but is parallel to the transform direction related to the relative motion between the Eurasia and Nubia plates. Therefore, the main question we address in the present study is: do transform faults related to the Eurasia/Nubia plate boundary exist in the Azores? Knowing that the main source of strain is related to plate kinematics, we conclude that the sinistral strike-slip NNW–SSE fault plane solution is not consistent with either the fault dip (ca. 65°, which is typical of a normal fault) or the ca. ENE–WSW direction of maximum extension; both are consistent with a normal fault, as observed in most major earthquakes on faults striking around NNW–SSE in the Azores. In contrast, the dextral strike-slip ENE–WSW fault plane solution is consistent with the transform direction related to the anticlockwise rotation of Nubia relative to Eurasia. Altogether, tectonic data, measured ground motion, observed destruction, and modelling are consistent with a dextral strike-slip source fault striking ENE–WSW. Furthermore, the bulk clockwise rotation measured by GPS is typical of bookshelf block rotations observed at the termination of such master strike-slip faults. Therefore, we suggest that the 1998 earthquake can be related to the WSW termination of a transform (ENE–WSW fault plane solution) associated with the Nubia–Eurasia diffuse plate boundary.

1. Introduction

The Central Azores Islands (Faial, Pico, S. Jorge, Graciosa and Terceira islands, Figs. 1 and 2) were born during the Quaternary at the Azores Triple Junction (ATJ), more specifically within the boundary between the Eurasia (Eu) and Nubia (Nu) plates. The ATJ is currently of the rift–rift–rift type. The Middle-Atlantic Rift makes the northern and southern arms, and the eastern arm is made of the Terceira Rift (TR), which connects to the Gloria Fault and the Azores Gibraltar Fault Zone in the east (Fig. 1). According to DeMets et al. (2010), there should be an Azores microplate interacting differently with the neighbouring Eu and Nu plates (Fig. 1): the Azores–Eu motion should be dextral oblique extension, and the Azores–Nu motion should be dextral strike-slip along an ENE–WSW direction. Based on GPS, tectonic and seismic data, Marques et al. (2013) concluded that the Nu–Eu boundary in the Azores is not discrete, and therefore the existence of an intervening Azores microplate is unlikely. Instead, the boundary is diffuse in its western half, with deformation accommodated by a ca. 150 km wide strip extending south of the western half of the TR. This has major implications in the distribution of strain, because maximum extension (approximately ENE–WSW) should be similar all over the diffuse boundary. The general structure in the diffuse boundary (Central Azores) is that of a sequence of WNW–ESE grabens and horsts (Fig. 2): the Graciosa and Terceira islands grew inside the TR; the Pico–Faial volcanic ridge sits on the master fault bounding the Faial Half-graben in the north; and the S. Jorge Island developed in the middle of a narrow graben, the S. Jorge Graben.

With the exception of the very small area of the islands (Fig. 1), the Azores crust lies below sea level, which is a strong limitation to directly observe and characterise deformation. Moreover, appreciable surface rupture related to main tectonic and M > 4 earthquakes has not been observed within the islands. Even if there were minor surface rupture, the superficial effects of very slow deformation imposed by the hyper-slow differential motion between Eurasia and Nubia (ca. 4 mm/yr) would not survive, because erosion, sedimentation and volcanic rates are much faster than the tectonic rate. For instance, Costa et al. (2014) and Hildenbrand et al. (2008, 2012a,b) have shown that major periods of massive island destruction (mostly large-scale landslides and flank

* Corresponding author. Tel.: +351 217500000; fax: +351 217500064.
E-mail address: fomarques@fc.ul.pt (F.O. Marques).

http://dx.doi.org/10.1016/j.tecto.2014.06.024
0040-1951/

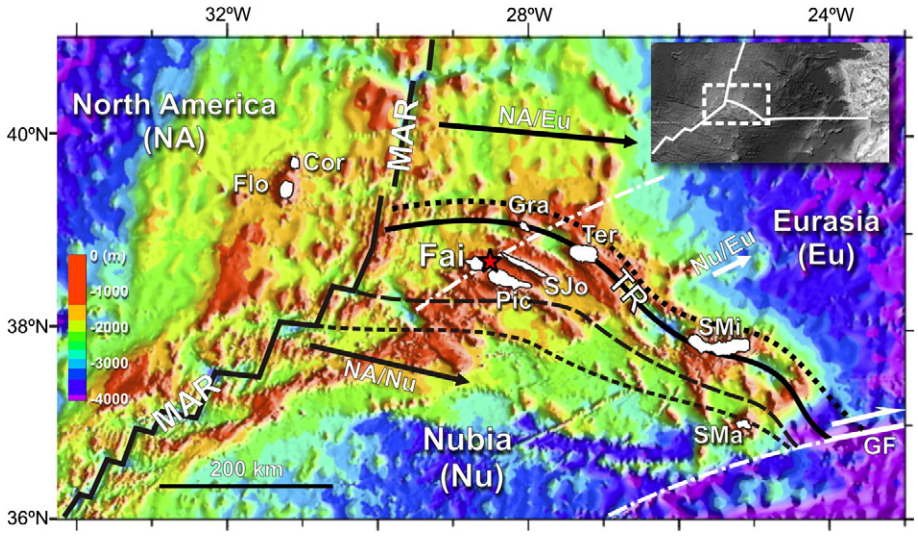

Fig. 1. Sketch of the general framework of the Azores Triple Junction. Black-rimmed red star marks the 1998 Faial earthquake. MAR and TR are the Mid-Atlantic and Terceira rifts, respectively. GF is the dextral strike-slip Gloria Fault. Full black arrows represent the velocity vectors of Eurasia (Eu) and Nubia (Nu) relative to North America (NA). Full white arrow represents the velocity vector of Eu relative to Nu. Dotted black line marks the northern shoulder of the TR, which represents the northern Nu/Eu plate boundary for both the diffuse boundary and the microplate scenarios. Black dashed and black long-dashed lines mark the southern boundaries of the hypothetical Azores microplate and the diffuse Nu/Eu plate boundary, respectively. White dash-dotted lines represent small circles around the MORVEL Nu/Eu pole (DeMets et al., 2010), which represent the transform direction related to the Nu/Eu boundary. From W to E, the Azores Islands are Flores (Flo), Corvo (Cor), Faial (Fai), Pico (Pic), S. Jorge (SJo), Graciosa (Gra), Terceira (Ter), S. Miguel (SMi), and Santa Maria (SMa).
Background image built with data retrieved from http://topex.ucsd.edu/marine_topo/mar_topo.html (Smith and Sandwell, 1997).

collapses) are intercalated with short periods of fast volcanic construction, which are able to mask intra-island evidence of the effects of large-scale tectonics occurring in the underlying plateau.

The Azores earthquakes show a few characteristics that make the 1998 Faial shock unique: (1) it has been reported since the early 1930s that very rare earthquakes (i.e. of tectonic origin, and M > 4) have seemingly occurred inside the islands (e.g. Agostinho, 1931; Borges et al., 2007; Machado, 1959). In fact, no major intra-island tectonic earthquake has been recorded in the Azores since earthquakes can be measured instrumentally. Locally, earthquakes occur inside the islands, but they are mostly related to volcanism rather than tectonics, which is the case, for instance, of the ongoing seismic crisis in the S. Miguel Island (e.g. Silva et al., 2012). (2) From a total of 24 major earthquakes for which the focal mechanisms have been computed (e.g. Borges et al., 2007), very few tectonic and M > 4 earthquakes are strike-slip (4 out of 24), and by far the large majority shows normal fault kinematics (16 out of 24) (e.g. Borges et al., 2007; Buforn et al., 1988, 2004; Grimison and Chen, 1988; Hirn et al., 1980; McKenzie, 1972; Miranda et al., 1998; Moreira, 1985; Udías et al., 1976 for a synthesis). (3) The main fault trends associated with tectonic M > 4 earthquakes are the WNW–ESE and NNW–SSE trends. The exception to this most common scenario can be the Faial 1998 shock, because deformation propagated inland, and the main source fault is pure strike-slip. Furthermore, this peculiar earthquake occurred within the Pico–Faial volcanic ridge (although close to the northern edge) and it can be related to a different trend (ENE–WSW), overlooked in the Azores, although of probable large-scale tectonic meaning as argued in the present paper. These characteristics, together with the relationship with plate kinematics and strains, support and justify the importance of studying the 1998 Faial shock.

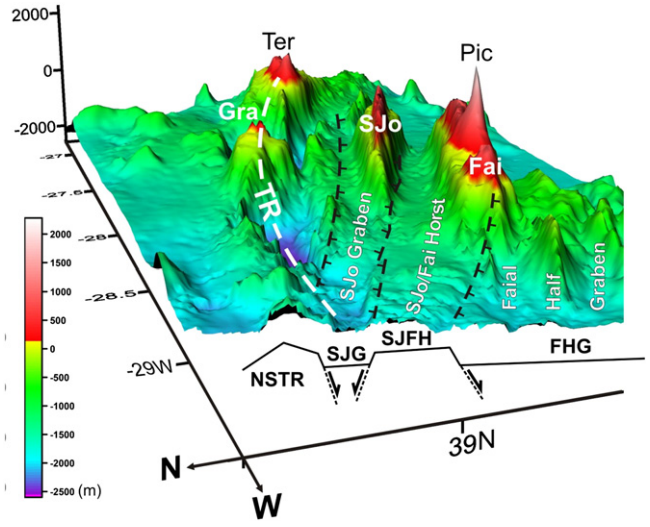

Fig. 2. 3D surface with interpreted main tectonic framework (viewed from WNW). TR is the Terceira Rift. Fai, Pic, SJo, Gra and Ter correspond to the islands of Faial, Pico, S. Jorge, Graciosa and Terceira, respectively.
3D surface built using topographic data available at http://w3.ualg.pt/~jluis/misc/ac_plateau1km.grd (Lourenço et al., 1998).

The TR is a ca. 620 km-long sigmoidal graben filled at regular spaces (ca. 80 km) by large-volume central volcanism making up islands and large seamounts (Fig. 1). Here we hypothesise that the regular spacing is due to concentrated volcanism at the intersection between the TR and transform faults related to the Nu/Eu plate boundary, thus making up privileged conduits. However, such transforms have never been recognised, which could be due in part to the low resolution of the bathymetry. Therefore, we looked for different evidence, in the form of earthquakes, like the 1998 Faial earthquake, which can be related to transform motion due to the Nu/Eu interaction in the Azores.

Given the premises and current knowledge outlined above, the questions we address in this article are: (1) which was the fault responsible for the earthquake? The sinistral NNW–SSE or the dextral ENE–WSW? (2) Which one is consistent (or inconsistent) with the known plate kinematics in the Azores? (3) What kind of fault is it? Are there transform faults associated with the Nu/Eu plate boundary? (4) What is the meaning of the measured ground deformation? (5) What are the sources of strain/stress? Our ultimate objective is a better understanding of strain (mostly faults) in the Azores Triple Junction, in terms of typology,

distribution, geometry, kinematics, earthquake generation and sources of stress.

In order to tackle these problems, we used: (1) a 50 m resolution DEM to evaluate the topography and interpret the main tectonic lineaments; (2) a detailed structural analysis to recognise and characterise the main faults, and interpret their tectonic meaning; (3) GPS data to measure, characterise and interpret the ground motion due to the main shock and subsequent aftershocks; (4) seismic data to characterise the main rupture and aftershocks in terms of position, nodal planes, and fault geometry and kinematics; and (5) modelling to test the consistency between fault plane solutions, aftershocks, tectonic data, and ground motion measured from GPS data.

2. Geological setting

Faial constitutes one of the emerged parts of a single volcanic ridge, the Pico–Faial Ridge, which is elongated along azimuth N110°. According to Hildenbrand et al. (2012a,b), Faial has three main volcanic complexes: a dismantled volcano older than ca. 850 ka, unconformably overlain by two volcanic complexes, one ca. 360 ka old, and another younger than ca. 120 ka. The most prominent tectonic feature in Faial is the central graben affecting the whole island. The fault scarps are clearly visible in the Faial Graben (Fig. 3), but the actual fault surfaces are only visible locally, mostly along sea cliffs. Faults and fault scarps strike N110°–120° on average, and faults dip steeply (60°–70°) to the NNE (in the S) or SSW (in the N). According to Hildenbrand et al. (2012a,b), the Faial Graben is younger than 360 ka.

The main geological features in the neighbourhood of the 1998 shock are the prominent Faial Graben in Faial Island, and the Pico Volcano (2351 m above sea level) in western Pico Island.

The 9th July 1998 earthquake (ML = 5.8) was shortly preceded by a 4.9 earthquake, and the combined effect of these two shocks impeded the adequate registration of the events by the local seismic network. Only 4 stations were able to record these events, and, as a consequence, the available hypocentre solution still has a great uncertainty, particularly the focal depth and the fault orientation (Matias et al., 2007). Following the main shock, thousands of aftershocks were recorded by the local seismic network in the following months. These data were used by Matias et al. (2007) to relocate the main aftershocks, recorded in the first 20 days following the main shock, by joint inversion of hypocentres and 1D velocity models. After relocation, the aftershocks present a complex shape, with the majority distributed along a main N–S direction, therefore making an angle >20° with one of the fault planes (N151°) of the centroid moment tensor (CMT, Harvard University) solution for the main shock. Refined hypocentral solutions, derived from 3D tomographic inversion, were later presented by Dias et al. (2007), with decreased spatial dispersion and showing an aftershock distribution in two main directions: N–S and ENE–WSW. In terms of focal depth, most aftershocks are located between 3 and 13 km, with shallower events occurring inland Faial. Events with focal depths less than 6 km occur in the NE sector of the island, associated with the main faults bounding the Faial Graben in the N.

Fernandes et al. (2002) used a set of GPS data acquired in 1997 and 1998 (one month after the main event) in a network of marks distributed all over Faial, in order to constrain the parameters that define the fault that generated the main shock. They analysed two solutions, the N61° dextral strike-slip, and the N151° sinistral strike-slip computed by CMT, and concluded that, from geodetic data and statistical criteria, it was not possible to decide for the strike direction of the main shock. Anyway, Fernandes et al. (2002) estimated the fault geometry for both hypotheses. In the model, triggering effects were not considered, resulting in poor model fit to the observations in NE and SW Faial. Neighbouring geodetic marks in NE Faial show opposite displacement directions, which were interpreted by Fernandes et al. (2002) as a possible interaction of the main rupture with the Faial Graben. In the present study we used tectonic and seismic data, and numerical modelling to show how the main shock interacted with the two master faults bounding the Faial Graben in the north.

Interferometric synthetic aperture radar (InSAR) was applied to the available set of ERS images, aimed at mapping the deformation resulting from the 1998 seismic crisis (Catita et al., 2005). Despite the adverse circumstances, mainly due to the reduced number of SAR images and large areas with vegetation, Catita et al. (2005) managed to build fringe patterns with approximately 3 cm of range change between 1992 and 1998. Although correlation breaks down in many areas, the fringe pattern is legible in NW Pico Island. The fringe pattern detected in this

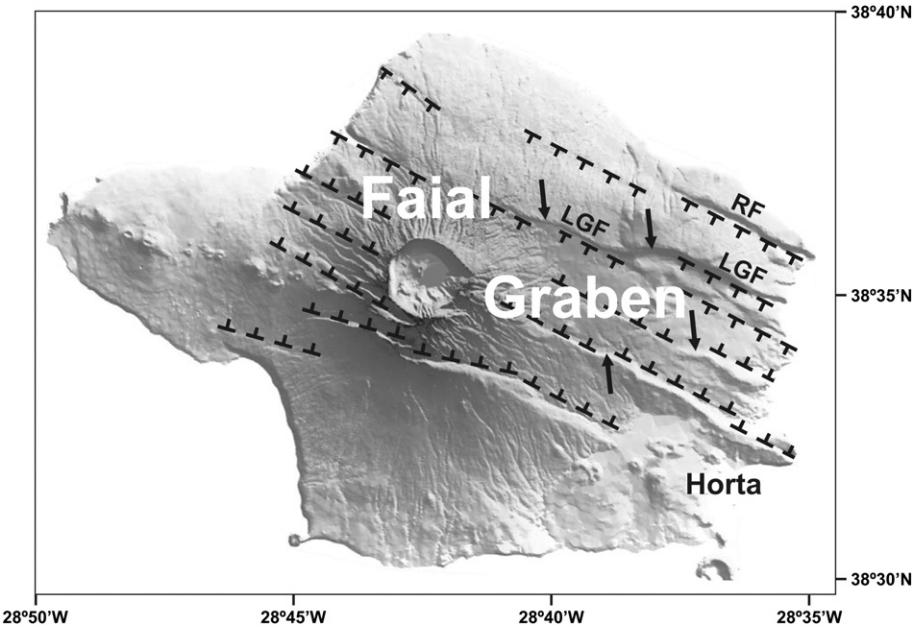

Fig. 3. Tectonic framework of the Faial Island, where the fault scarps making up the Faial Graben stand out. RF — Ribeirinha Fault. LGF — Lomba Grande Fault. Arrows mark bends (in plan view) on normal faults, which indicate a sinistral strike-slip component. Lighting from NE.

part of Pico can be related to the synthetic model computed from the fault parameters of Fernandes et al. (2002) (see Fig. 9), and Catita et al. (2005) concluded that the observed interferometric fringes generally agree with the synthetic models and, therefore, are coherent with the available seismic and GPS data.

3. Data

3.1. GPS velocities

A dense geodetic network was installed on the islands of Faial and Pico, in the early years of the 20th century. The network was first surveyed with GPS, on regular campaigns, in 1995 (Pico Island) and 1997 (Faial). In 1998, one month after the earthquake, the network was again surveyed with GPS, but only occupying 32 stations (29 on Faial and 3 on Pico). All the surveys were performed with dual-frequency GPS receivers, collecting data every 15 s and occupying stations for 1 to 4 h. The mean baseline length between stations is ca. 3000 m.

The GPS data were analysed and processed by Fernandes et al. (2002) using Bernese software. The mean position of the geodetic marks was estimated by least squares adjustment of the GPS baselines, fixing the position of FAIM station (in Horta) on the three campaigns. The displacement field was calculated as the difference between the estimated coordinates for the 32 stations in 1995, 1997 and in 1998. The displacement vectors are shown in Fig. 4.

3.2. Main earthquake and aftershocks

The CMT solution for the Faial earthquake (Figs. 5 and 6D) shows the existence of two nodal planes where the main shock may have occurred: N61° (ENE–WSW) and N151° (NNW–SSE). The fault plane solution indicates vertical dip and almost pure strike-slip motion in both faults: left-lateral in the NNW–SSE fault, and right-lateral in the ENE–WSW fault.

The relocation of aftershocks with the 3D tomographic model (Dias et al., 2007, and this work) (Fig. 5) shows a pattern that is only seemingly simple to interpret. Relocated aftershocks also show the reactivation of the two WNW–ESE main faults making up the northern boundary of the Faial Graben. Two main trends strike approximately orthogonal to each other: one ENE–WSW (blue line in Fig. 5), and the other NNW–SSE (yellow line in Fig. 5). However, both trends are composed of two main concentrations of aftershocks: (1) one offshore (where the main shock occurred) that trends ENE–WSW, and the other onshore trending WNW–ESE and reactivating the northernmost faults of the Faial Graben. (2) The NNW–SSE trend shows two concentrations of aftershocks, both offshore: one in the south, more linear and striking ca. N175° (black line in Fig. 5), and the other in the north and approximately circular. Both NNW–SSE and ENE–WSW trends show a wide distribution of aftershocks, not the discrete linear concentration expected for single and vertical faults (the CMT solution for the Faial earthquake). Therefore, we made three seismic sections across the two main trends to find the dip of the main faults (Fig. 6). The seismic sections show an ENE-WSW fault dipping ca. 80° to the SSE (Fig. 6B), a NNW–SSE fault dipping ca. 65° to the WSW (Fig. 6C), and a WNW–ESE fault (Faial Graben) dipping ca. 65° to the SSW (Fig. 6A). The NNW–SSE and WNW–ESE faults have the typical dip of normal faults, while the ENE–WSW fault dips steeply like a strike-slip fault.

3.3. Seismic intensity

As shown by the isoseismal maps in Matias et al. (2007), Oliveira et al. (2012), Senos et al. (1998) and Zonno et al. (2010), the main destruction occurred in Faial, especially in the NE corner of the island where destruction was maximal (Fig. 7). In contrast, damage in Pico and S. Jorge islands was reduced or even minimal, and mainly concentrated on the capital village in westernmost Pico, and confined to a small village in WNW S. Jorge.

4. Co-seismic modelling/GPS data inversion

The co-seismic displacements were determined by coordinate difference of the GPS surveys carried out in 1995 (Pico, 3 geodetic marks), 1997 (Faial, 29 geodetic marks) (Catalão et al., 2006), and 1998 (in the same geodetic marks, one month after the earthquake), assuming that there were no other significant volcanic or seismic events in those periods. For more detailed information see Fernandes et al. (2002).

The spatial distribution of the observations is asymmetric relative to the ENE–WSW fault plane, with few observations on the northern block. Moreover, the epicentre is in the ocean, on the northern flank of the Pico–Faial Ridge, and so does most of the rupture surface. According to the isoseismal information, the earthquake was weakly felt in S. Jorge Island (NE of Faial), with minimal observed damage only in the NW

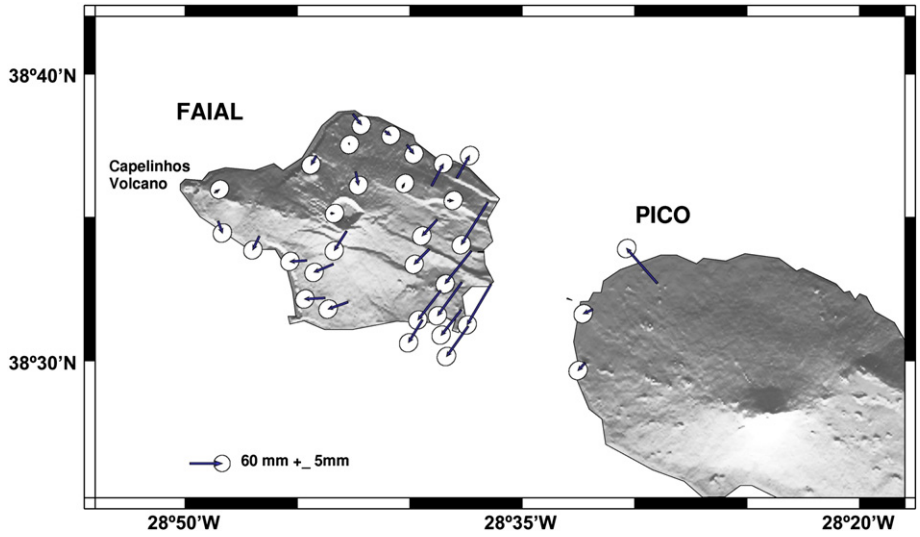

Fig. 4. The measured displacements (blue arrows) show three main features: (1) clockwise rotation of the island southwest of the fault that bounds the Faial Graben in the N (RF). (2) Opposite displacements to south and north of the RF fault in NE Faial. (3) Counter clockwise rotation of western Pico. GPS surveyed in 1997 and 1998.

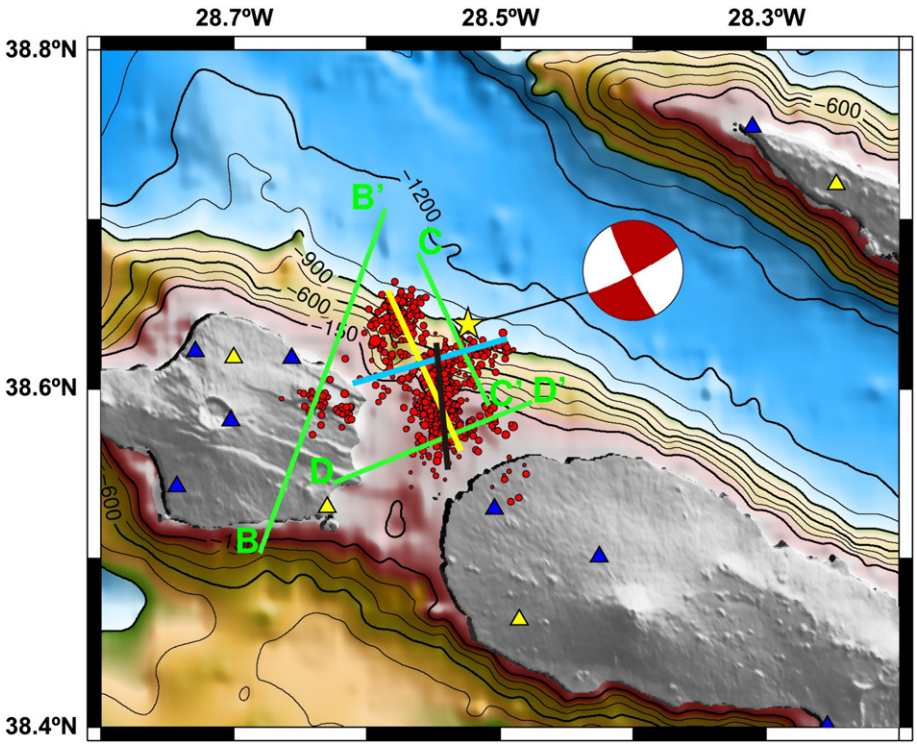

Fig. 5. Map with location of the main shock (yellow star) and respective fault plane solution (beach-ball, from Borges et al., 2007), representation of the relocated aftershocks (red dots), seismic stations (blue and yellow triangles, the latter used to locate the main shock), and the seismic profiles shown in Fig. 6. The yellow, black and blue full lines represent the N155°, N175° and N75° possible fault planes. Background DEM of the islands built from topographic data supplied by Instituto Geográfico do Exército (IGeoE, Portugal), with vertical and horizontal resolutions of 10 m and 50 m, respectively.
Background bathymetry from Lourenço et al. (1998), with 100 m resolution.

sector of the island (e.g. Matias et al., 2007); therefore, we can assume that there was negligible deformation in S. Jorge.

In order to constrain the mathematical model, we used: (1) the measured ground motion (Fernandes et al., 2002); (2) the direction and dip of the faults inferred from the seismic data (this study); (3) the structural data regarding onshore faults where seismicity was observed (Hildenbrand et al., 2012a,b); (4) the depth estimated from the seismic data (Dias et al., 2007; Matias et al., 2007); (5) the earthquake magnitude (Borges et al., 2007; Matias et al., 2007) to estimate the corresponding rupture surface (e.g. Wells and Coppersmith, 1994, their Fig. 16); and (6) the line of sight deformation measured with SAR interferometry (Catalão et al., 2011; Catita et al., 2005). The inclusion of these measurements in the model results in a directional and positional constraint for the estimated fault parameters of the main shock. Contrary to previous studies (Dias et al., 2007; Fernandes et al., 2002; Matias et al., 2007), in this study we assume that the main event interacted with the fault system of the Faial Graben, causing displacement on its northern faults, as observed in the aftershocks. The problem is the actual kinematics of these faults: the main component is that of normal faults, but the horizontal component is not obvious. From the bends marked with arrows in Fig. 3, we can deduce a left-lateral strike-slip component, which is in agreement with the bookshelf structure expected at the termination of a strike-slip fault or fault rupture (e.g. Lin et al., 2010; Ron et al., 1986, their Figure 6).

We modelled the observed coseismic displacement using a rectangular model fault, along which the displacement is uniform and the top is parallel to the Earth's surface, according to Okada's (1985) algorithm. An elastic, homogeneous and isotropic half-space with a rigidity of 30 GPa was assumed. The inversion was done using the non-linear generalised inverse algorithm developed by Briole et al. (1986), which estimates the parameters of the fault and fault plane displacement that best fit the GPS data. The fault parameters were estimated using weighted least squares inversion of the east and north displacement vectors, with the data weighted by the reciprocal of the square of the

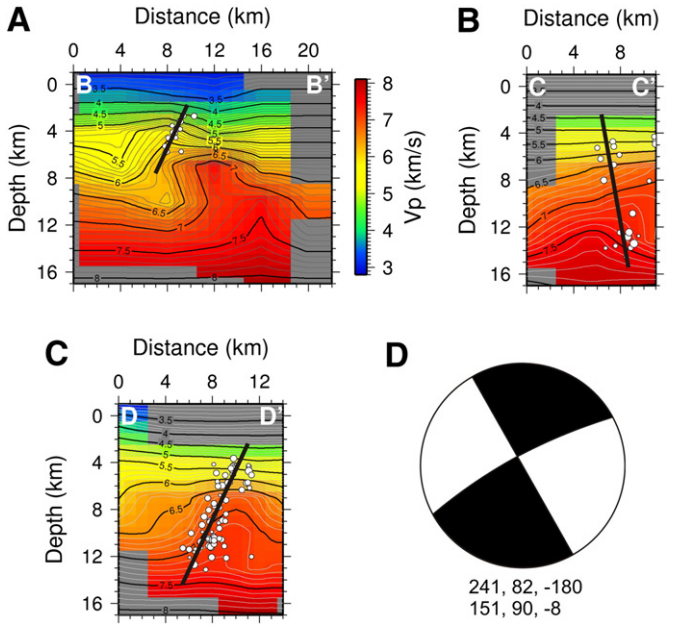

Fig. 6. A, B and C — Seismic profiles B–B′, C–C′ and D–D′, respectively, showing the distribution of aftershocks at depth, overlying the tomographic model of Dias et al. (2007). Inferred faults are represented by black full lines. D — Fault plane solution according to the CMT solution of Harvard University.

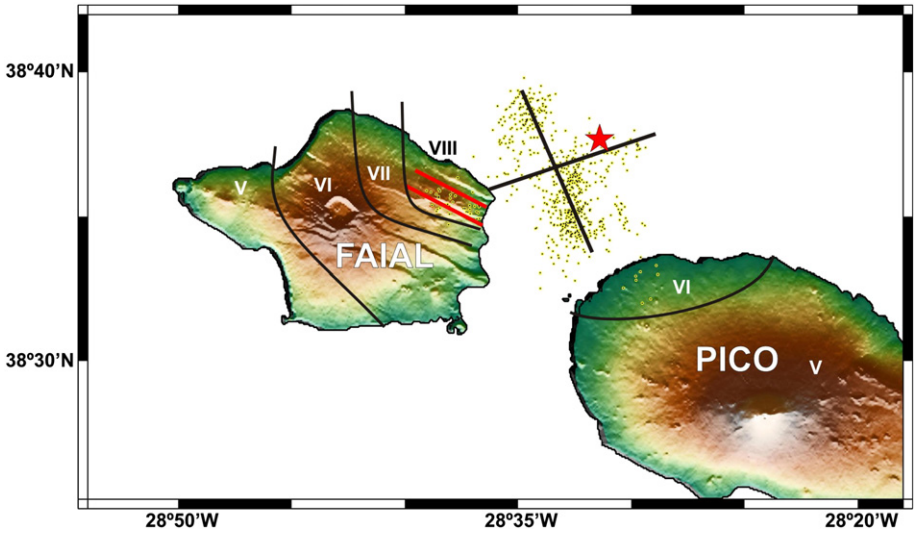

Fig. 7. Macroseismic intensity (modified Mercalli scale) inferred for the Faial and Pico islands (modified after Senos et al., 1998). Red star marks the location of the 1998 Faial main shock. Black straight lines represent the nodal planes. Red lines mark the faults in the Faial Graben where aftershocks occurred. Yellow-rimmed black dots represent the relocated aftershocks.

estimated error. The estimated error for each campaign is between 1 mm and 7 mm for the horizontal component (with an average of 4 mm), and between 3 and 14 mm for the vertical component.

The inversion process was performed in three steps. (1) In the first step, we used the initial solution given in the CMT catalogue and estimated the 8 parameters describing the fault of the main event (location, depth, length, width, strike, dip, strike-slip, dip-slip) by changing the original position of the epicentre (latitude, longitude, depth) supplied by SIVISA, which is feasible considering the uncertainties of ca. 5 km associated with that solution (Matias et al., 2007). Given the geological setting, the ground motion, and the isoseismal distribution, we considered for the initial solution the ENE–WSW right lateral fault (fault 1a in Table 1). (2) In the second step, the residuals of the first inversion (computed as the difference between GPS and modelled displacements) were used to estimate the parameters of the two northernmost main faults of the Faial Graben: the Ribeirinha and Lomba Grande faults, which strike N120° and dip 60°–70° to the SSW (Hildenbrand et al., 2012a,b). The evidence of the displacement on these structures is given in Figs. 5 and 6. Some of the relocated seismic events are shallow events (about 4 km) and inside the island. In the inversion process, some of the parameters of these two faults were constrained: the position, and strike and dip obtained by field measurements (Hildenbrand et al., 2012a,b); the depth of the fault (ca. 4 km given in Dias et al., 2007), and the length estimated by the trace at the surface. (3) In the third step, the position, direction and size of the three faults were fixed, and the slip parameters estimated on a single system of equations. The results are shown in Table 1. The measure of misfit, given by the reduced chi-square, was computed as the ratio between the weighted residual sum of squares and degrees of freedom (number of data − number of parameters). The reduced chi-square was determined for the 3-fault model solution based on the data uncertainties (10 mm for the horizontal and 21 mm for the vertical), and on the number of 32 stations and 9 parameters. For this model the reduced chi-square was 1.8. A misfit of 1 would indicate that the residuals are statistically consistent with the data errors. In this case we have assumed that data uncertainties are too optimistic, and we decided to scale the uncertainties by two (~1.8). The obtained reduced chi-square is now 1.06. If we assume only the main event, and using the same data uncertainties, the misfit increases to 1.4, meaning that this fault model does not fit the physical phenomenon as well as the proposed 3-fault model.

The optimal uniform-slip dislocation closely follows the displacement measured in the field, and is consistent with the alignment of aftershocks. Furthermore, this 3-fault model is able to reproduce the measured dislocation in NE Faial. In this model, the largest surface deformation occurs onshore NE Faial, as confirmed by the high level of destruction in this area (e.g. Oliveira et al., 2012). The geodetic moment magnitude is Mw = 6.18, consistent with the CMT catalogue. The surface projections of the three dislocations are shown in Figs. 8 and 9. They closely follow the coseismic events relocated by Dias et al. (2007).

Following the same procedure, we also modelled the two other possible solutions, as indicated by the CMT fault plane solutions and the aftershock sequence: the long N155° sinistral strike-slip fault (fault 1c in Table 1, and red in Fig. 10), and the short N175° sinistral strike-slip fault (fault 1b in Table 1, and green in Fig. 10).

5. Discussion

The motions between Azores–Eurasia (dextral oblique extension) and Azores–Nubia (dextral strike-slip), shown by DeMets et al. (2010) in a scenario with an Azores microplate, have to be reconfigured in a

Table 1
Fault parameters determined from inversion of GPS data. Depth refers to the top of the fault.

Fault	Length (km)	Width (km)	Dip (°)	Strike (°)	Lat (°N)	Lon (°W)	Depth (km)	Dip-slip (cm)	Strike slip (cm)	Kinematics
1a	12	5.5	83	264	38.6184	28.5550	5	0	−117	Dextral
1b	6	5.5	89	175	38.5964	28.5446	4	0	147	Sinistral
1c	10.6	5.5	89	155	38.6118	28.5597	4	0	99	Sinistral
2	2	1	70	118	38.5986	28.6306	2	15	0	Normal/sinistral
3	2.2	1	70	118	38.5932	28.6573	2	34	14	Normal/sinistral

Using the same data uncertainties, the reduced chi-square is: fault 1a = 1.06; fault 1b = 1.6; and fault 1c = 2.15.

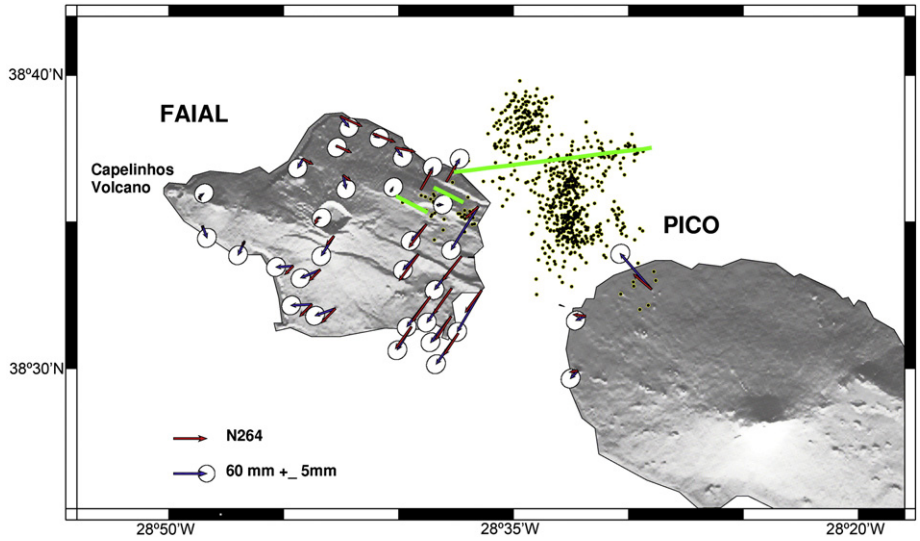

Fig. 8. Comparison of measured and modelled station displacements for the 3-fault model, with the main ENE–WSW fault. Blue arrows: displacement measured with GPS. Red arrows: modelled displacement. Red lines: faults.

scenario without the Azores microplate (Marques et al., 2013). The TR seems to be taking up most of the oblique extension, as shown by the prominent graben comprising the TR; therefore, the dextral strike-slip motion (transform motion) should be taking place south of the TR, where the boundary with Nubia is diffuse. Here, as in the case of the Faial 1998 earthquake, the transform direction works as a dextral strike-slip fault, similarly to the Gloria Fault (GF in Fig. 11), as expected from the counter clockwise rotation of Nubia relative to Eurasia.

The aftershock sequence shows two main lineaments, from which we infer the position and geometry of two main faults making an angle of ca. 90° between them (ENE–WSW and NNW–ESE). However, classical rock mechanics predicts conjugate faults at an angle of ca. 60°. Therefore, we infer that the faults should be the result of a more complex stress field or of mixing of structures inherited from the MAR with structures generated by the Nu/Eu kinematics. Two main fault systems have been recognised in the Azores (WNW–ESE and NNW–SSE), and a third is being proposed in the present work (ENE–WSW) (Fig. 11): (1) the best-known fault system in Central Azores strikes WNW–ESE, which is responsible for the horst–graben structure shown in Fig. 2. (2) The NNW–SSE fault system could be generated by the differential motion between Eurasia and Nubia, and work as pure normal as shown by most of the available fault plane solutions. (3) The ENE–WSW fault system has not been recognised in the Azores, but it is predicted by the plate velocities reported in DeMets et al. (2010), and in the fault plane solutions of major earthquakes (e.g. Borges et al., 2007; Hirn et al., 1980). The transform direction is produced by the rotation of Nubia relative to Eurasia, and changes strike along the TR, as shown by the plate velocity configuration in the Azores (DeMets et al., 2010). Locally, as in the case of the Faial 1998 earthquake, the transform direction works as a dextral strike-slip fault, similarly to the Gloria Fault (Fig. 11), as expected from the counter clockwise rotation of Nubia relative to Eurasia.

The NNW–SSE faults in the Azores, dipping to the WSW or ENE, are typically normal faults according to the fault plane solutions available (cf. Figure 8 in Borges et al., 2007). This is consistent with the relative motion between Eu and Nu (DeMets et al., 2010), because the NNW–SSE trend is orthogonal to the principal extension in the diffuse Nu/Eu

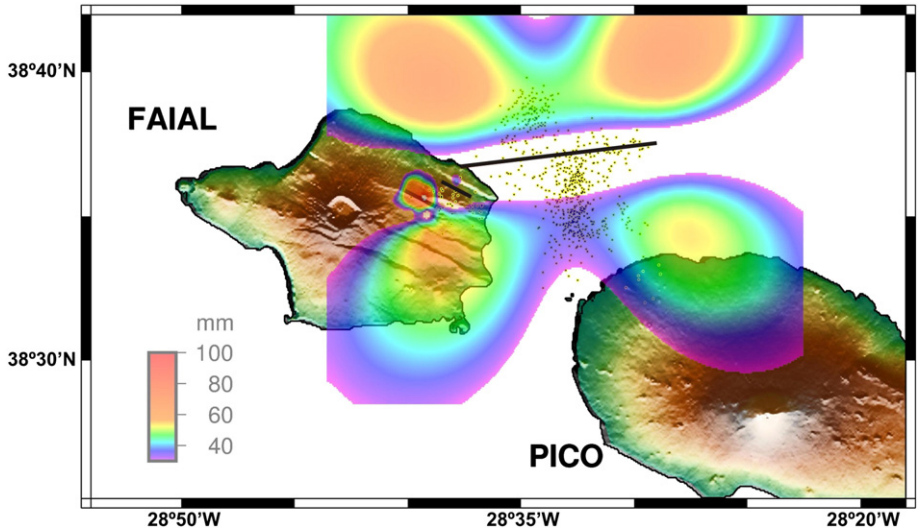

Fig. 9. Comparison of model fault location (represented by thick red lines) and seismic events (represented by yellow-rimmed black dots). Coloured overlay is modelled station displacements for the 3-fault model.

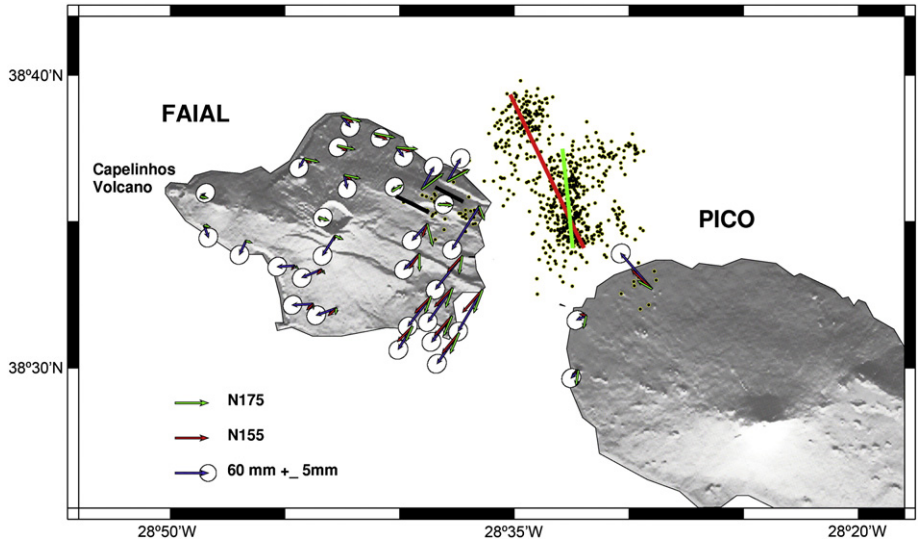

Fig. 10. Comparison of measured and modelled station displacements for a 3-fault model, with a main short N175° sinistral strike-slip fault (green), or a main long N155° sinistral strike-slip fault (red). Note that: (1) the long N155° fault model solution cannot reproduce the measured ground displacement (black arrows), with displacement directions everywhere at high angle to the measured displacement; and (2) the short N175° fault model solution cannot reproduce the measured ground displacement, with displacement magnitude everywhere much smaller than the measured displacements.

boundary. Given that the two NNW–SSE fault plane solutions correspond to normal faults, it is not relevant if the normal fault dips to the ENE or to the WSW; it is normal fault in any case. In contrast, when the fault plane solution shows two vertical pure strike-slip faults, one sinistral (striking NNW–SSE) and the other dextral (striking ENE–WSW), then a problem of consistency arises: the NNW–SSE fault strikes orthogonal to the maximum extension, and thus should not be a pure strike-slip fault; it should be a pure normal fault, as observed when the two fault plane solutions trend NNW–SSE and dip around 65°. In fact, the NNW–SSE fault inferred from the 1998 Faial aftershock sequence dips ca. 65°, which means that it is consistent with normal faulting. The alternative, which is the main thesis of the present paper, is that the main shock occurred on the fault corresponding to the fault plane solution that trends ENE–WSW, which is coincident with the transform direction related to the rotation of Nu relative to Eu in the Azores, and therefore consistent with plate kinematics and induced strain. Similarly to the Gloria Fault (Fig. 11), the faults trending ENE–WSW should be vertical and pure dextral strike-slip.

Two main features stand out from the measured velocity field in Faial (Fig. 4): (1) the opposite velocities in Faial's NE corner, to each side of the RF and LGF faults, and (2) the concentric velocities in central Faial. The possible kinematics of the faults making up the Faial Graben (WNW–ESE) are: (1) pure normal (as observed in fault plane solutions of major earthquakes in the Azores); (2) normal/dextral as inferred from the angular relationship between fault strike (WNW–ESE) and direction of maximum extension (ENE–WSW) (Fig. 11); and (3) normal/sinistral if there is clockwise bookshelf rotation related to the differential motion between NA/Eu and NA/Nu. Note that the sinistral strike-slip component is consistent with the release bends shown in Fig. 3. As shown by modelling, the velocities in NE Faial can only be explained if there is oblique displacement on the northernmost faults of the Faial Graben, i.e. only if a sinistral strike-slip component is

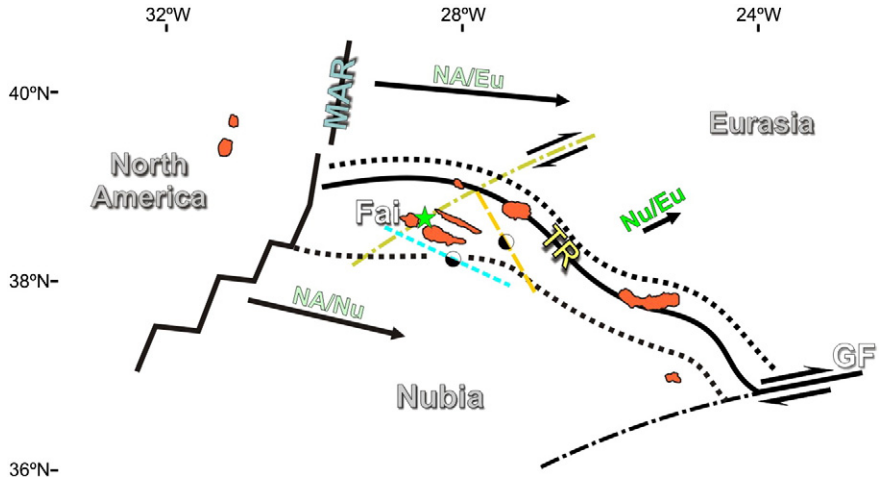

Fig. 11. Schematic representation of plate distribution and kinematics (arrows with reference to the involved plates, DeMets et al., 2010), Nu/Eu boundary (marked by dotted black lines), the small circles related to rotation of Nu relative to Eu (dash-dot lines), and main fault systems (NNW–SSE marked by long-dashed yellow line; WNW–ESE marked by dashed blue line; ENE–WSW marked by dash-dot green line). Strike-slip kinematics indicated by black half arrows, and normal fault kinematics indicated by half white/half black circles. MAR and TR represent the Mid-Atlantic and Terceira rifts, respectively.

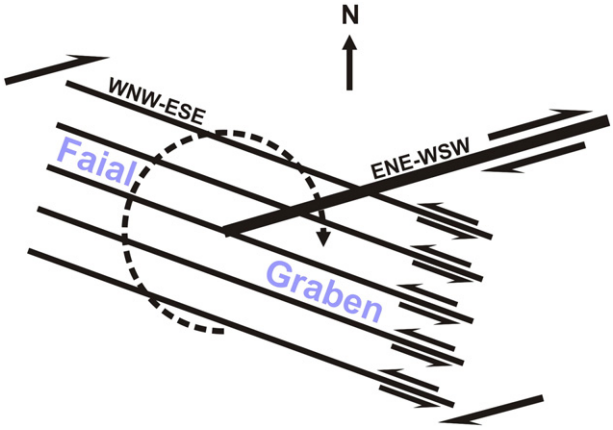

Fig. 12. Sketch with kinematic interpretation of the measured ground motions and estimated movement on the main fault. Note that the WNW–ESE fault system (making the Faial Graben and sketched here) works as a bookshelf in response to the observed clockwise rotation imposed by the dextral movement in the main ENE–WSW fault.

added to the main normal component, which is consistent with the tectonics inferred from fault geometry. Although not clearly reproduced in the model, the concentric velocity field in central Faial can be explained if the Faial Graben corresponds to the termination of the ENE–WSW dextral strike-slip fault (Fig. 12). Similar fault and kinematic configurations (block rotations associated with the termination of strike-slip faults) have been observed and reported by Ron et al. (1986), and measured by GPS by Lin et al. (2010). Noticeably, the prominent faults onshore Faial are not visible offshore in the channel between Faial and Pico islands (Figure 4 in Tempera, 2009). This is consistent with our hypothesis of a fault termination, because in such a configuration the displacement on the WNW–ESE graben faults is attenuated by the displacement on the ENE–WSW fault. In contrast, it is not consistent with the N175° fault, because there is no direct interaction with the Faial Graben faults.

The continuation of the ENE–WSW fault to the ENE, toward the TR, is not clear. On the one hand, its strike may be affected by the local stress field imposed by the massive Pico stratovolcano, deflecting it toward a more E–W trend. On the other hand, there is no clear evidence of the fault trace on the available bathymetry. However, in the nearby S. Jorge Island (to the ENE of the epicentre) there is a clean-cut jump in GPS velocities in the middle of the island (Marques et al., 2013; Mendes et al., 2013), which could be explained by an ENE–WSW transform. GPS velocities in Figure 5a and c in Marques et al. (2013) show that there is dextral strike-slip motion along a line passing where the 1998 shock occurred and through the middle of the S. Jorge Island (Fig. 13). Coincidently, this line is the transform direction predicted by Morvel for this region, and also the direction of one of the fault plane solutions of the Faial 1998 shock, the ENE–WSW fault.

The N75° fault inferred from the aftershock sequence is at a small angle to the local transform direction, which is closer to ENE–WSW in the Faial area (DeMets et al., 2010). Based on the radial stress field that develops around conical loads (e.g. Duran, 2000; Marques and Cobbold, 2002, 2006), we argue that the N75° strike is a local deflection of the general ENE–WSW transform direction, due to stresses born at the massive Pico stratovolcano (Fig. 13). Such stresses could also be responsible for the southwards dip of the N75° fault, by addition of a vertical component of compression to the far field stresses.

According to the CMT fault plane solutions, the main rupture may have occurred on two fault planes, the ENE–WSW or the NNW–SSE. The aftershocks also occurred along two main lineaments, which strike ca. N75° and N175°. From a geophysical point of view, the main shock may have occurred on either of the two faults. However, the numerical modelling using the three possible main faults (N155° long sinistral fault, N175° short sinistral fault, and N84° dextral fault), constrained by the aftershock sequence (Figs. 8 and 10), indicates that: (1) the long N155° fault model solution is not consistent with the measured ground displacement, because displacement directions are everywhere at a high angle to the measured displacement (Fig. 10). (2) The short N175° fault model solution cannot reproduce the measured ground displacement, because displacement magnitude is everywhere much smaller than the measured displacement (Fig. 10). (3) The N84° model fault is the one that best reproduces the measured displacements, in both direction and magnitude (Fig. 8). Furthermore: (1) the major destruction was observed in NE Faial, to the W of the epicentre. (2) The N175° fault deduced from the seismicity alignment shows no spatial interaction with the Faial Graben faults (Fig. 13). (3) The N175° fault can only generate an M ~ 6 event if we assume either that the fault extends to the north (with the NW cluster deviated from it), or that the fault ruptures the entire crust (which has a thickness here of ~14 km according to Dias et al., 2007). The proposed ENE–WSW fault has the

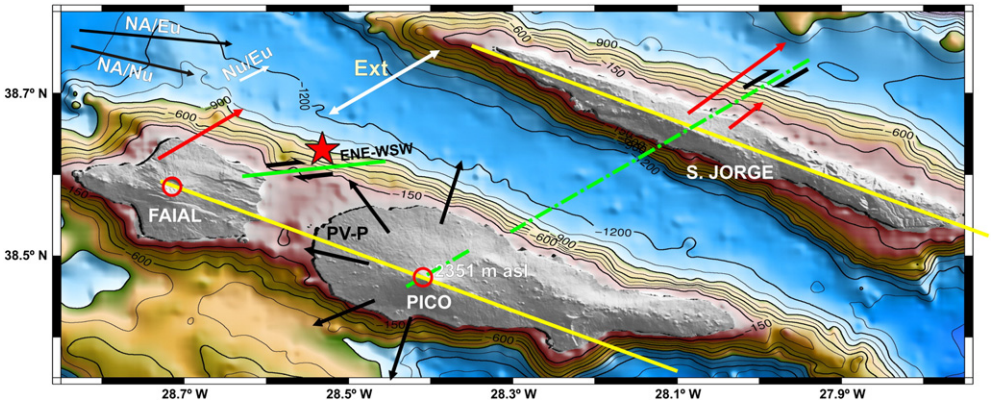

Fig. 13. Schematic representation of the main volcano/tectonic structures and GPS velocities. Note that the ENE–WSW fault (green full line) is aligned with the main volcano in Faial (Caldera Volcano, red circle), and that the line separating the jump in GPS velocities in S. Jorge (green dash-dot line, which represents a small circle around the MORVEL Nubia–Eurasia pole — DeMets et al., 2010) is aligned with the Caldera in the Pico Volcano (red circle). The yellow lines through the main volcanoes in Pico–Faial and S. Jorge ridges are the surface expressions of the main tectonic horst/graben structure in the basement (Fig. 2). The red arrows correspond to the GPS velocities with fixed Pico (Marques et al., 2013). It seems therefore that the main volcanoes in the Pico–Faial Ridge developed at the intersection between the WNW–ESE and the ENE–WSW fault systems. Morvel plate velocities (DeMets et al., 2010) are represented at the top-left corner. Black full arrows represent the radial stresses induced by the Pico volcano on the surrounding lithosphere. Black half arrows indicate fault kinematics. The red star marks the location of the Faial 1998 earthquake. PV-P is the topographic force exerted by the Pico Volcano, a volcanic cone with top at 2351 m above sea level (asl).

advantage of not requiring a rupture of the entire crust. (4) Last but most importantly, the Morvel plate velocities and the GPS velocities shown in Figure 5 of Marques et al. (2013) and reproduced in Fig. 13 are not consistent with a pure strike-slip motion on the NNW–SSE fault, because maximum extension is orthogonal to the fault plane. In fact, most of the ca. NNW–SSE fault plane solutions for tectonic earthquakes with M > 4 have normal fault kinematics (cf. Borges et al., 2007), as expected from the known plate kinematics (ENE–WSW extension). Putting all data together, we conclude that the main shock occurred on the ENE–WSW fault. Knowing that the ENE–WSW fault is approximately along the transform direction related to the Nu/Eu plate boundary, we conclude that the fault responsible for the 1998 Faial earthquake strikes ENE–WSW and can be a transform associated with the TR.

The differences between measured ground motion and model velocities can be the result of model insufficiencies, mostly flat surface (therefore lack of island topography effects), rigidity in the model, and small number of faults in the model as compared to nature. The fact that the NNW–SSE aftershock sequence is more prominent than the ENE–WSW is not, by itself, guarantee that the main shock occurred on a NNW–SSE fault. In fact, stress triggering has become a common observation. For instance, the 1992 M = 7.4 Landers earthquake changed the failure stress on the southern San Andreas fault system (King et al., 1994; Stein et al., 1992). Similarly, many other earthquakes have been triggered by its predecessors (e.g. Freed, 2005; Stein, 1999; Stein et al., 1994, 1997 for a review). We conclude that the concentration of aftershocks along the N175° fault could well mean that it readjusted to motion along the N75° fault during the main earthquake.

From the complex geometry of the aftershock pattern and continued seismicity from 1998 to present-day, the aftershock swarm could well correspond to volcanic seismicity triggered by the main earthquake and subsequent aftershocks.

6. Conclusions

The fault plane solution and the aftershock sequence of the 1998 Faial earthquake in the Azores show that the main shock occurred on two possible vertical faults striking NNW–SSE (sinistral strike-slip) and ENE–WSW (dextral strike-slip). Given that the main earthquake and aftershocks occurred within the diffuse Nu/Eu plate boundary, and that the maximum extension there is approximately orthogonal to the NNW–SSE fault plane solution, we conclude that the vertical and sinistral strike-slip NNW–SSE solution is inconsistent with the known plate kinematics in the Azores. There, the main earthquakes on faults trending close to NNW–SSE, for which the focal mechanisms are known, show that the faults are neither vertical nor strike-slip; they dip like classical normal faults, and have the kinematics of normal faults. In contrast, the ENE–WSW fault is sub-vertical and dextral strike-slip, thus consistent with the rotation of Nu relative to Eu and the transform direction in the diffuse Nu/Eu boundary. Therefore, we conclude that the main earthquake occurred on the ENE–WSW fault, which is a transform related to the Nu/Eu diffuse boundary.

The tectonics observed onshore Faial, the measured displacements, and the observed destruction, all point to the ENE–WSW fault as the source fault of the 1998 Faial earthquake, and therefore corroborate the conclusion reached from plate kinematics and strain. The dextral clockwise motion and clockwise rotation measured by GPS are typical of block rotations associated with the termination of strike-slip faults. Based on the known plate kinematics, fault geometry and kinematics, we conclude that the ENE–WSW dextral strike-slip fault can be a transform associated with the Nubia–Eurasia plate boundary.

The numerical three-fault models used to test the consistency of the possible fault planes with the measured ground displacement indicate that the ENE–WSW dextral strike-slip fault is the best-fitting solution.

Acknowledgements

This is a contribution to projects TEAMINT (POCTI/CTE/48137/2002) and MEGAHazards (PTDC/CTE-GIX/108149/2008) funded by FCT, Portugal. We thank the two anonymous reviewers for the comments that helped to substantially improve the final manuscript.

References

Agostinho, J., 1931. The volcanoes of the Azores Islands. Bull. Volcanol. 8, 123–138.
Borges, J.F., Bezzeghoud, M., Buforn, E., Pro, C., Fitas, A., 2007. The 1980, 1997 and 1998 Azores earthquakes and some seismo-tectonic implications. Tectonophysics 435, 37–54.
Briole, P., De Natale, G., Gaulon, R., Pingue, F., Scarpa, R., 1986. Inversion of geodetic data and seismicity associated with the Friuli earthquake sequence (1976–1977). Ann. Geophys. 4, 481–492.
Buforn, E., Udías, A., Colombás, M.A., 1988. Seismicity, source mechanisms and seismotectonics of the Azores–Gibraltar plate boundary. Tectonophysics 152, 89–118.
Buforn, E., Bezzeghoud, M., Udías, A., Pro, C., 2004. Seismic sources on the Iberia–African plate boundary and their tectonic implications. Pure Appl. Geophys. 161, 623–646.
Catalão, J., Miranda, J.M., Lourenco, N., 2006. Deformation associated with the Faial (Capelinhos) 1957–1958 eruption: inferences from 1937–1997 geodetic measurements. J. Volcanol. Geotherm. Res. 155, 151–163.
Catalão, J., Nico, G., Hanssen, R., Catita, C., 2011. Merging GPS and atmospherically corrected InSAR data to map 3D terrain displacement velocity. IEEE Trans. Geosci. Remote Sens. 49, 2354–2360. http://dx.doi.org/10.1109/TGRS.2010.2091963.
Catita, C., Feigl, K.L., Catalão, J., Miranda, J.M., Victor, L.M., 2005. InSAR time series analysis of the 9th July 1998 Azores earthquake. Int. J. Remote Sens. 26. http://dx.doi.org/10.1080/01431160512331337835.
Costa, A.C.G., Marques, F.O., Hildenbrand, A., Sibrant, A.L.R., Catita, C.M.S., 2014. Large-scale flank collapses in a steep volcanic ridge: Pico-Faial Ridge, Azores Triple Junction. J. Vol. Geotherm. Res. 272, 111–125.
DeMets, C., Gordon, R.G., Argus, D.F., 2010. Geologically current plate motions. Geophys. J. Int. 181, 1–80.
Dias, N.A., Matias, L., Lourenço, N., Madeira, J., Carrilho, F., Gaspar, J.L., 2007. Crustal seismic velocity structure near Faial and Pico Islands (Azores), from local earthquake tomography. Tectonophysics 445, 301–317.
Duran, J., 2000. Sands, Powders, and Grains: An Introduction to the Physics of Granular Materials. Springer-Verlag, New York (214 pages).
Fernandes, R.M.S., Miranda, J.M., Catalão, J., Luis, J.F., Bastos, L., Ambrosius, B., 2002. Coseismic displacements of the Mw = 6.1, July 9, 1998, Faial earthquake (Azores, North Atlantic). Geophys. Res. Lett. 29. http://dx.doi.org/10.1029/2001GL014415.
Freed, A., 2005. Earthquake triggering by static, dynamic and postseismic stress transfer. Annu. Rev. Earth Planet. Sci. 33, 335–367.
Grimison, N., Chen, W., 1988. The Azores–Gibraltar plate boundary: focal mechanisms, depths of earthquakes and their tectonic implications. J. Geophys. Res. 91, 2029–2047.
Hildenbrand, A., Madureira, P., Marques, F.O., Cruz, I., Henry, B., Silva, P., 2008. Multi-stage evolution of a sub-aerial volcanic ridge over the last 1.3 Myr: S. Jorge Island, Azores Triple Junction. Earth Planet. Sci. Lett. 273, 289–298.
Hildenbrand, A., Marques, F.O., Catalão, J., Catita, C.M.S., Costa, A.C.G., 2012a. Large-scale active slump of the SE flank of Pico Island (Azores). Geology 40, 939–942.
Hildenbrand, A., Marques, F.O., Costa, A.C.G., Sibrant, A.L.R., Silva, P.F., Henry, B., Miranda, J. M., Madureira, P., 2012b. Reconstructing the architectural evolution of volcanic islands from combined K/Ar, morphologic, tectonic, and magnetic data: the Faial Island example (Azores). J. Volcanol. Geotherm. Res. 241–242, 39–48.
Hirn, A., Haessler, J., Hoang Trong, P., Wittlinger, G., MendesVictor, L., 1980. Aftershock sequence of the January 1st, 1980 earthquake and present-day tectonics in the Azores. Geophys. Res. Lett. 7, 501–504.
King, G.C.P., Stein, R.S., Lin, J., 1994. Static stress changes and the triggering of earthquakes. Bull. Seismol. Soc. Am. 84, 935–953.
Lin, K.-C., Hu, J.-C., Ching, K.-E., Angelier, J., Rau, R.-J., Yu, S.-B., Tsai, C.-H., Shin, T.-C., Huang, M.-H., 2010. GPS crustal deformation, strain rate, and seismic activity after the 1999 Chi-Chi earthquake in Taiwan. J. Geophys. Res. 115, B07404. http://dx.doi.org/10.1029/2009JB006417.
Lourenço, N., Miranda, J.M., Luis, J.F., Ribeiro, A., Victor, L.A.M., Madeira, J., Needham, H.D., 1998. Morpho-tectonic analysis of the Azores Volcanic Plateau from a new bathymetric compilation of the area. Mar. Geophys. Res. 20 (3), 141–156.
Machado, F., 1959. Submarine pits of the Azores plateau. Bull. Volcanol. 21, 109–116.
Marques, F.O., Cobbold, P.R., 2002. Topography as a major factor in the development of arcuate thrust belts: insights from sandbox experiments. Tectonophysics 348, 247–268.
Marques, F.O., Cobbold, P.R., 2006. Effects of topography on the curvature of fold-and-thrust belts during shortening of a 2-layer model of continental lithosphere. Tectonophysics 415, 65–80.
Marques, F.O., Catalão, J.C., DeMets, C., Costa, A.C.G., Hildenbrand, A., 2013. GPS and tectonic evidence for a diffuse plate boundary at the Azores Triple Junction. Earth Planet. Sci. Lett. 381, 177–187.
Matias, L., Dias, N.A., Morais, I., Vales, D., Carrilho, F., Madeira, J., Gaspar, J., Senos, L., Silveira, A., 2007. The 9th of July 1998 Faial Island (Azores, North Atlantic) seismic sequence. J. Seismol. 11, 275–298.
McKenzie, D., 1972. Active tectonics of the Mediterranean region. Geophys. J. R. Astron. Soc. 30, 109–185.
Mendes, V.B., Madeira, J., Brum da Silveira, A., Trota, A., Elosegui, P., Pagarete, J., 2013. Present-day deformation in São Jorge Island, Azores, from episodic GPS measurements (2001–2011). Adv. Space Res. 51, 1581–1592.

Miranda, J.M., Mendes Victor, L., Simoes, J.Z., Luis, J.F., Matías, L., Shimamura, H., Shiobara, H., Nemoto, H., Mochizuki, H., Hirn, A., Lepine, J.C., 1998. Tectonic setting of the Azores Plateau deduced from OBS survey. Mar. Geophys. Res. 20, 171–182.
Moreira, V.S., 1985. Seismotectonics of Portugal and its adjacent area in the Atlantic. Tectonophysics 117, 85–96.
Okada, Y., 1985. Surface deformation due to shear and tensile faults in a half space. Bull. Seismol. Soc. Am. 75, 1135–1154.
Oliveira, C.S., Ferreira, M.A., Mota-de-Sá, F., Neves, F., 2012. The concept of a disruption index: application of the overall impact of the July 9, 1998 Faial earthquake (Azores Islands). Bull. Earthq. Eng. 10, 7–25.
Ron, H., Aydin, A., Nur, A., 1986. Strike-slip faulting and block rotation in the Lake Mead fault system. Geology 14, 1020–1023.
Senos, M.L., Gaspar, J.L., Cruz, J., Ferreira, T., Nunes, J.C., Pacheco, J.M., Alves, P., Queiroz, G., Dessai, P., Coutinho, R., Vales, D., Carrilho, F., 1998. O terramoto do Faial de 9 de Julho de 1998. 1° Simpósio de Meteorologia e Geofísica da APMG, Lagos, Portugal, pp. 61–67.
Silva, R., Havskov, J., Bean, C., Wallenstein, N., 2012. Seismic swarms, fault plane solutions, and stress tensors for São Miguel Island central region (Azores). J. Seismol. 16, 389–407.
Smith, W.H.F., Sandwell, D.T., 1997. Global seafloor topography from satellite altimetry and ship depth soundings. Science 277, 1957–1962.
Stein, R.S., 1999. The role of stress transfer in earthquake occurrence. Nature 402, 605–609.
Stein, R.S., King, G.C.P., Lin, J., 1992. Change in failure stress in southern San Andreas fault system caused by the 1992 Magnitude = 7.4 Landers earthquake. Science 258, 1328–1332.
Stein, R.S., King, G.C.P., Lin, J., 1994. Stress triggering of the 1994 M = 6.7 Northridge, California, earthquake by its predecessors. Science 265, 1432–1435.
Stein, R.S., Barka, A.A., Dieterich, J.H., 1997. Progressive failure on the Northern Anatolian Fault since 1939 by earthquake stress triggering. Geophys. J. Int. 128, 594–604.
Tempera, F., 2009. Benthic Habitats of the Extended Faial Island Shelf and Their Relationship to Geologic, Oceanographic and Infralittoral Biologic Features(PhD. Thesis) University of St. Andrews, Scotland, UK.
Udías, A., López Arroyo, A., Mézcua, J., 1976. Seismotectonics of the Azores–Alboran region. Tectonophysics 31, 259–289.
Wells, D.L., Coppersmith, K.J., 1994. New empirical relationships among magnitude, rupture length, rupture width, rupture area, and surface displacement. Bull. SSA 84, 974–1002.
Zonno, G., Oliveira, C.S., Ferreira, M.A., Musachio, G., Meroni, F., Mota-de-Sá, F., Neves, F., 2010. Assessing seismic damage through stochastic simulation of ground shaking: the case of the 1998 Faial earthquake (Azores Islands). Surv. Geophys. 31, 361–381.